

Regular article

A non-orthogonal Kohn-Sham method using partially fixed molecular orbitals

Kazushi Sorakubo, Takeshi Yanai, Kenichi Nakayama, Muneaki Kamiya, Haruyuki Nakano, Kimihiko Hirao

Department of Applied Chemistry, School of Engineering, University of Tokyo, Tokyo 113–8656, Japan

Received: 24 February 2003 / Accepted: 2 June 2003 / Published online: 16 September 2003
© Springer-Verlag 2003

Abstract. A density functional theory method using partially fixed molecular orbitals (PFMOs) is presented. The PFMOs, which have some fixed molecular orbital coefficients and are non-orthogonal, are a generalization of the extreme localized orbitals (ELMOs) of Couty, Bayse, and Hall (1997) *Theor Chem Acc* 97:96. A non-orthogonal Kohn-Sham method with these PFMOs is derived, and is applied to molecular calculations on the ionization potential of pyridine, the energy difference between *cis*- and *trans*-butadiene, the reaction barrier height of the cyclobutene-*cis*-butadiene interconversion, and the potential energy curve of the hydrogen shift reaction of hydroxycarbene to formaldehyde. The PFMO Kohn-Sham method reproduces well the results of the full Kohn-Sham method without having a restriction on the molecular orbital coefficients. The difference is less than 0.1 eV in the ionization potential and about 0.1 kcal/mol in the barrier height and in the potential energy calculations.

Keywords: Non-orthogonal Kohn-Sham method – Partially fixed molecular orbital (PFMO) – Extreme localized molecular orbital (ELMO)

Introduction

The description of the electronic structure of large molecular systems is one of the central issues in current quantum chemistry. Much effort has been expended in this area at the correlated level as well as at the Hartree-Fock (HF) level.

At the correlated level in *ab initio* molecular orbital (MO) theory, the local correlation method is one of the most successful methods. It is widely known that the

canonical HF orbitals are usually spread over the whole system, and consequently, electron pairs are not spatially well separated. However, physically, dynamic electron correlation in the molecular environment is a short-range effect approaching r^{-6} in the long-distance limit. To make use of the short-range nature in the electron correlation method, the use of spatially localized molecular orbitals (LMOs) is essential. There have been a number of papers on local correlation methods [1], including the local second-order Møller-Plesset (LMP2) method [1, 2, 3, 4, 5, 6, 7], the local coupled cluster doubles (LCCD) method [8], the local coupled cluster singles and doubles (LCCSD) method [9, 10], and the local coupled cluster singles and doubles with perturbative triples (LCCSD(T)) method [11].

At the HF level, linear scaling methods (or methods that move toward linear scaling) have been intensely studied. In each part of the self-consistent field (SCF) procedure, techniques for approaching linear scaling have been developed. For example, such techniques include the fast multipole moment (FMM) method [12, 13], the tree code method [14, 15], and the *J*-matrix engine [16] for the Coulomb part of the Fock matrix; the order-*N*-exchange (ONX) [17], linear-exchange-*K* [18], and near-field-exchange (NFX) [19] methods for the exchange part of the Fock matrix; and the conjugate gradient density matrix search to avoid diagonalization of the Fock matrix [20]. This area of study is attracting the interests of quantum chemists, and the development of appropriate techniques is still under intense investigation.

An HF method has been proposed by Couty et al. [21], which also utilizes LMOs. The LMOs of Couty et al., *extremely localized molecular orbitals (ELMOs)*, are defined as MOs that have coefficients only on some predetermined basis functions and no coefficients on the other functions. Thus, the ELMOs are essentially non-orthogonal to each other. The SCF scheme proceeds via the quasi-Newton-Raphson method [22], keeping the localizability of the orbitals without diagonalization

Correspondence to: Haruyuki Nakano; Takeshi Yanai
e-mail: nakano@qcl.t.u-tokyo.ac.jp; yanai@qcl.t.u-tokyo.ac.jp

of the Fock matrix, since the iterative diagonalization of the Fock matrix is no longer considered to be a good strategy for the non-orthogonal orbitals.

The HF method of Couty et al. has been successfully applied to the molecular systems and is a candidate for large system theory. However, the HF method does not include correlation effects. Moreover, the constraints on the MOs described in the paper are so severe, that the total energy has an error of several millihartrees even for small molecules with a few atoms, and so it is compensated for by mixing of the MOs after carrying our SCF scheme [21].

In the present article, we extend the HF method of Couty et al. to a Kohn-Sham (KS) density functional theory (DFT) method that uses non-orthogonal orbitals, such as ELMOs. We also generalize the ELMOs to more flexible MOs, denoted as partially fixed molecular orbitals (PFMOs), which have some fixed MO coefficients for the predetermined basis functions. Our method is applied to molecular calculations on pyridine, butadiene, cyclobutene, and hydroxycarbene. The performance of the new non-orthogonal KS-DFT method using the PFMOs is comparable to the original KS-DFT method using orthogonal unfixed MOs. The errors in the total energy are in the order of millihartrees, and those in the relative energy, such as the ionization and activation energies, are within one millihartree.

The contents of the present article are as follows. In the next section, the non-orthogonal KS-DFT method is derived and the PFMOs are introduced. In the subsequent section, the criteria for fixing the MO coefficients are described and then the scheme is tested on some molecular systems. In the final section, concluding remarks are given.

Theory

Non-orthogonal Kohn-Sham DFT method

We will begin by deriving a non-orthogonal Kohn-Sham DFT method. The non-orthogonal KS method is parallel to the ELMO HF method. In the following, we will therefore not explain the details that are common to the ELMO HF method.

Let $\{\chi_\mu\}$ be basis functions and $\{\phi_{ij}\}$ be the non-orthogonal MOs of the system,

$$\phi_i = \sum_{\mu} C_{\mu i} \chi_{\mu} \quad (1)$$

Using these non-orthogonal MOs, the KS energy is written as

$$E = \sum_{ij} 2h_{ij}^{\text{core}} S_{ij}^{-1} + \sum_{ijkl} (ij|kl) \left(2S_{ij}^{-1} S_{kl}^{-1} - C_{\text{ex}} S_{ik}^{-1} S_{jl}^{-1} \right) + E_{\text{xc}}[\rho] \quad (2)$$

where S_{ij} , h_{ij}^{core} , and $(ij|kl)$ are the overlap, bare nuclei, and electron repulsion integrals in the MO basis, defined by

$$S_{ij} = \int d\mathbf{r} \phi_i(\mathbf{r}) \phi_j(\mathbf{r}) \quad (3)$$

$$h_{ij}^{\text{core}} = \int d\mathbf{r} \phi_i(\mathbf{r}) \left(-\frac{\nabla^2}{2} - \sum_{\alpha} \frac{Z_{\alpha}}{|\mathbf{r} - \mathbf{R}_{\alpha}|} \right) \phi_j(\mathbf{r}) \quad (4)$$

and

$$(ij|kl) = \int d\mathbf{r}_1 d\mathbf{r}_2 \phi_i(\mathbf{r}_1) \phi_j(\mathbf{r}_1) \frac{1}{r_{12}} \phi_k(\mathbf{r}_2) \phi_l(\mathbf{r}_2) \quad (5)$$

respectively. C_{ex} is a constant for the hybrid DFT method. The last term in Eq. 2, $E_{\text{xc}}[\rho]$, is an exchange-correlation energy functional for the electronic density $\rho(\mathbf{r})$, which is defined in the local density approximation as

$$E_{\text{xc}}[\rho] = \int d\mathbf{r} f(\rho) \quad (6)$$

and in the generalized gradient approximation as

$$E_{\text{xc}}[\rho] = \int d\mathbf{r} f(\rho, \Delta\rho) \quad (7)$$

The total electronic energy, Eq. 2, is dependent the expansion coefficients $\{C_{\mu i}\}$ through Eq. 1. The KS orbitals are determined such that the coefficients minimize the energy expression, Eq. 2.

In the conventional KS-DFT, we obtain the orthogonal KS orbitals through the iterative diagonalization of the KS matrix \mathbf{f}^{KS} , that is, the solution of the KS-SCF equation,

$$\mathbf{f}^{\text{KS}} \mathbf{C} = \mathbf{S} \mathbf{C} \epsilon \quad (8)$$

where \mathbf{C} and ϵ store the MO coefficients and orbital energies, respectively, and \mathbf{S} is the overlap matrix in the AO basis. On the other hand, in the KS method using non-orthogonal orbitals, as well as the HF method using ELMOs, the diagonalization procedure is not available. Hence, we employ the quasi-Newton-Raphson (QNR) scheme for orbital optimization [21, 22] instead. The QNR scheme scales as N^2 (N : the size of the system), whereas the diagonalization scheme scales as N^3 . Another advantage of the QNR scheme is that it allows us, not only to treat non-orthogonal MOs, but also to fix some MO coefficients as in the ELMOs and the partially fixed MOs described in the subsequent sub-section. Neither diagonalization, nor manipulation of the full coefficients is necessary.

The Newton-Raphson equation has the form,

$$\delta\mathbf{X} = \mathbf{X}^{i+1} - \mathbf{X}^i = -\mathbf{H}^{-1}\mathbf{g} \quad (9)$$

where \mathbf{X} is a one-dimensional array that stores the active MO coefficients, and \mathbf{g} and \mathbf{H} are the gradient vector and the Hessian matrix, respectively, for the energy E with respect to active MO coefficients,

$$g_{\alpha k} = \frac{\partial}{\partial C_{\alpha k}} E \quad (10)$$

and

$$h_{\alpha k, \beta l} = \frac{\partial^2}{\partial C_{\alpha k} \partial C_{\beta l}} E \quad (11)$$

In the quasi-Newton-Raphson method, the true Hessian matrix is not used, but instead, an approximation of the Hessian matrix at the current iteration is employed. In our implementation, following the ELMO HF procedure, the blocked Hessian matrix,

$$h_{\alpha k, \beta l} \cong \begin{cases} \frac{\partial^2}{\partial C_{\alpha k} \partial C_{\beta k}} E & (k = l) \\ 0 & (k \neq l) \end{cases} \quad (12)$$

and its inverse are computed analytically at the initial iteration, and the inverse Hessian matrix is updated after each iteration by the Broyden-Fletcher-Goldfarb-Shanno (BFGS) method [23].

In this way, we can optimize orbitals (keeping some MO coefficients fixed if necessary). Below, we provide explicit formulae for the gradient vector and the blocked Hessian matrix.

Gradient vector and approximate Hessian matrix

The KS energy Eq. (1) can be partitioned into the HF-like energy E'_{HF} and the exchange-correlation energy $E_{\text{xc}}[\rho]$ as

$$E = E'_{\text{HF}} + E_{\text{xc}}[\rho] \quad (13)$$

The former part E'_{HF} can be represented by

$$E'_{\text{HF}} = \sum_{\mu\nu} \left(h_{\mu\nu}^{\text{core}} + F_{\mu\nu}^{\text{HF}} \right) P_{\mu\nu} \quad (14)$$

where $h_{\mu\nu}^{\text{core}}$, $F_{\mu\nu}^{\text{HF}}$, and $P_{\mu\nu}$ are the bare-nuclei Hamiltonian integrals, the Fock-like matrix, and the density matrix in the AO basis, respectively. The Fock-like and density matrices are defined by

$$F_{\mu\nu}^{\text{HF}} = h_{\mu\nu}^{\text{core}} + \sum_{\sigma\tau} P_{\sigma\tau} [2(\mu\nu|\sigma\tau) - C_{\text{ex}}(\mu\tau|\sigma\nu)] \quad (15)$$

and

$$P_{\mu\nu} = \sum_{ij}^{\text{occ}} C_{\mu i} C_{\nu j} S_{ij}^{-1} \quad (16)$$

where $S_{ij} = \sum C_{\mu i} C_{\nu j} S_{\mu\nu}$. The density function $\rho(\mathbf{r})$ and its gradient $\nabla\rho(\mathbf{r})$ in the latter part $E_{\text{xc}}[\rho]$ are represented in terms of the density matrix $P_{\mu\nu}$ as

$$\rho(\mathbf{r}) = 2 \sum_{\mu\nu} P_{\mu\nu} \chi_{\mu}(\mathbf{r}) \chi_{\nu}(\mathbf{r}) \quad (17)$$

and

$$\nabla\rho(\mathbf{r}) = 2 \sum_{\mu\nu} P_{\mu\nu} (\chi_{\nu}(\mathbf{r}) \nabla\chi_{\mu}(\mathbf{r}) + \chi_{\mu}(\mathbf{r}) \nabla\chi_{\nu}(\mathbf{r})) \quad (18)$$

From the expressions, Eqs. 13, 14, 15, 16, 17, 18, we can derive the gradient and Hessian formulae.

Differentiating the HF-like energy part E'_{HF} and the exchange-correlation energy part $E_{\text{xc}}[\rho]$, we find

$$\frac{\partial}{\partial C_{\alpha k}} E'_{\text{HF}} = \sum_{\mu\nu} 2F'_{\mu\nu} \frac{\partial P_{\mu\nu}}{\partial C_{\alpha k}} \quad (19)$$

and

$$\frac{\partial}{\partial C_{\alpha k}} E_{\text{xc}}[\rho] = \int d\mathbf{r} \frac{\partial\rho}{\partial C_{\alpha k}} \frac{\delta f(\rho)}{\delta\rho} = \sum_{\mu\nu} 2 \left[\int d\mathbf{r} \chi_{\mu} \frac{\delta E_{\text{xc}}}{\delta\rho} \chi_{\nu} \right] \frac{\partial P_{\mu\nu}}{\partial C_{\alpha k}} \quad (20)$$

Thus, we have the gradient formula,

$$\frac{\partial}{\partial C_{\alpha k}} E = \sum_{\mu\nu} 2f_{\mu\nu}^{\text{KS}} \frac{\partial P_{\mu\nu}}{\partial C_{\alpha k}} \quad (21)$$

with

$$f_{\mu\nu}^{\text{KS}} = F'_{\mu\nu} + \int d\mathbf{r} \chi_{\mu}(\mathbf{r}) \frac{\delta E_{\text{xc}}}{\delta\rho} \chi_{\nu}(\mathbf{r}) \quad (22)$$

The gradient for the density matrix $\partial P_{\mu\nu}/\partial C_{\alpha k}$ can be found elsewhere [21].

In a similar manner, we can further derive the initial blocked Hessian matrix,

$$\frac{\partial^2}{\partial C_{\alpha k} \partial C_{\beta k}} E = \frac{\partial^2}{\partial C_{\alpha k} \partial C_{\beta k}} E'_{\text{HF}} + \frac{\partial^2}{\partial C_{\alpha k} \partial C_{\beta k}} E_{\text{xc}}[\rho] \quad (23)$$

Since E'_{HF} is structurally close to the HF energy, we can use the same approximation as in the ELMO HF case. Neglecting the product of the first derivative of the density matrix, $(\partial P_{\mu\nu}/\partial C_{\alpha k})(\partial P_{\sigma\tau}/\partial C_{\beta k})$, we have [21]

$$\frac{\partial^2}{\partial C_{\alpha k} \partial C_{\beta k}} E'_{\text{HF}} \cong \sum_{\mu\nu} 2F'_{\mu\nu} \left(\frac{\partial^2 P_{\mu\nu}}{\partial C_{\alpha k} \partial C_{\beta k}} \right) \quad (24)$$

Similarly, we can derive the second derivative of $E_{\text{xc}}[\rho]$ as

$$\begin{aligned}
\frac{\partial^2}{\partial C_{\alpha k} \partial C_{\beta k}} E_{\text{xc}}[\rho] &= \int d\mathbf{r} \frac{\partial^2 \rho}{\partial C_{\alpha k} \partial C_{\beta k}} \frac{\delta f(\rho)}{\delta \rho} \\
&+ \int d\mathbf{r} \frac{\partial \rho}{\partial C_{\alpha k}} \frac{\partial \rho}{\partial C_{\beta k}} \frac{\delta^2 f(\rho)}{\delta \rho^2} \\
&\cong \int d\mathbf{r} \frac{\partial^2 \rho}{\partial C_{\alpha k} \partial C_{\beta k}} \frac{\delta f(\rho)}{\delta \rho} \\
&= \sum_{\mu\nu} 2 \left[\int d\mathbf{r} \chi_{\mu} \frac{\delta E_{\text{xc}}}{\delta \rho} \chi_{\nu} \right] \frac{\partial^2 P_{\mu\nu}}{\partial C_{\alpha k} \partial C_{\beta k}}
\end{aligned} \tag{25}$$

Here, the product of the first derivatives of density $(\partial\rho/\partial C_{\alpha k})(\partial\rho/\partial C_{\beta k})$ is neglected. From Eqs. 24 and 25, we have an approximate blocked Hessian matrix,

$$\frac{\partial^2}{\partial C_{\alpha k} \partial C_{\beta k}} E \cong \sum_{\mu\nu} 2 f_{\mu\nu}^{\text{KS}} \left(\frac{\partial^2 P_{\mu\nu}}{\partial C_{\alpha k} \partial C_{\beta k}} \right) \tag{26}$$

The second derivative of the density matrix $\partial^2 P_{pq}/\partial C_{\alpha k} \partial C_{\beta k}$ is further approximated for simplicity in the calculations, and this too, is given elsewhere [21].

Partially fixed molecular orbitals (PFMOs)

We then extend the definition of ELMOs. In the ELMO HF method, the MOs are forced to have non-zero elements only over a limited number of basis functions and are fully optimized with this localization constraint. In other words, this definition of an ELMO can be taken to mean that some MO coefficients are fixed at zero in the linear combination of the atomic orbitals (AOs),

$$\varphi_i = \sum_{\mu} C_{\mu i} \chi_{\mu} \tag{27}$$

($C_{\mu i} = 0$ for predetermined AO labels μ). This is quite effective for localizing orbitals, as there is no contribution from the AOs other than the predetermined AOs. However, since this is such a severe constraint, the error in the total energy reaches several millihartrees, even for small molecules such as, CH_4 , H_2O , and NH_3 . In fact, Couty et al. introduced the Jacobi correction to compensate for it [21].

Therefore, in our method, the condition that *some MO coefficients are fixed at zero* is relaxed to the condition that *some coefficients are fixed to certain values*,

$$\varphi_i = \sum_{\mu} C_{\mu i} \chi_{\mu} \tag{28}$$

where $C_{\mu i} = \text{fixed value}$ for predetermined AO labels μ . Although we have relaxed the MO condition, the computational scheme of the ELMO HF method is still applicable to our case. Now that the orbitals are not necessarily *extremely localized*, hereafter we call the

orbitals defined by Eq. 28 *partially fixed molecular orbitals* (PFMOs).

In the ELMO method of Couty et al., some predetermined variables are fixed at zero and thus do not affect the electronic density. On the other hand, in our method, some predetermined MO coefficients are also fixed, but they can assume non-zero values. Therefore, they contribute to the electronic density and energy. Note that, however, this does not reduce computational efficiency compared to the ELMO case.

Applications to molecular systems

We applied the present method to some molecular systems to illustrate its performance. The examples chosen are the ionization potential of pyridine, the energy difference between *cis*- and *trans*-butadiene, the reaction barrier height for the interconversion of cyclobutene and *cis*-butadiene, and the potential energy curve of the hydrogen shift reaction of hydroxycarbene to formaldehyde. The results are compared to those of the conventional KS-DFT method.

Since we have extended the concept of the ELMO to the PFMO in the previous section, we first describe a new scheme for fixing the coefficients of the PFMOs.

Some modern basis sets, such as Dunning's cc-pVXZ ($X = \text{D, T, Q, 5, \dots}$) [24] and the ANO [25] basis sets, consist of functions corresponding to atomic orbitals and other functions. For example, the cc-pVDZ basis set for carbon has functions corresponding to the $1s$, $2s$, and $2p$ atomic orbitals, functions for expressing the distortion of the valence orbitals, and functions describing polarization. For convenience, let us name the basis functions corresponding to the core atomic orbitals *core basis functions* and those corresponding to the valence atomic orbitals *valence basis functions*, and the other basis functions *extended basis functions*. [Note that only the functions corresponding to the atomic orbitals (e.g., the carbon $2s$ or $2p$), and not the functions for distortion, are *valence basis functions*].

The core and valence basis functions extracted from the original basis set constitute a minimal basis set. Using this minimal basis set, we first carry out a preliminary HF calculation, which can be readily performed in many cases, even for large molecules. According to the HF MOs solved for the minimal basis set, the fixed values are determined as follows:

1. The chemical core MOs. All the MO coefficients are frozen to the minimal basis set values.
2. The occupied MOs except for the core MOs.
 - (i) The coefficients of the core basis functions are frozen to the minimal basis set values.
 - (ii) The coefficients of the valence basis functions are frozen to the minimal basis set values if the absolute values of the coefficients are below a threshold δ .

- (iii) The criterion determining the coefficients of the extended basis functions is somewhat complicated. The basis functions are grouped by function center. If the absolute values of the coefficients of the *valence* basis functions in a group are all below the threshold δ , then the coefficients of the *extended* basis functions in the group are all frozen to zero. In other words, if the valence basis functions in a group are not important for an MO, then the extended basis functions in the group are also unimportant.

All the other variables are optimized in the PFMO KS calculations.

Note that MOs determined with this scheme are examples of PFMOs and other restrictions are possible. In fact, a different scheme will be necessary for inorganic compounds, particularly including transition metals.

The following provides some more details specific to the computations carried out.

We used the cc-pVDZ and cc-pVTZ basis sets with the polarization functions omitted. (Hereafter, we will label these VDZ and VTZ, respectively). The inclusion of the polarization functions is possible according to above Criterion (2-iii), but the reason for freezing them is a little weak, when compared to the extended functions for distortion of the valence orbitals. Thus, we omitted the polarization functions in the present test applications.

As reference orbitals for determining the fixed values through Criteria (1) and (2) mentioned above, we tested two types of HF orbitals built with the minimal basis set: the canonical MOs and the Boys localized MOs [26]. In this section, for brevity, we call these orbitals the canonical reference and localized reference MOs, respectively. We set the threshold of Criterion (2-ii) as $\delta = 0.001$ in all the computations.

Unless otherwise specified, a combination of the Becke 1988 exchange [27] and the one-parameter progressive correlation [28], a BOP functional, was used in

the KS-DFT calculations. The accuracy of the BOP functional is now well established [29, 30, 31].

Ionization potential of pyridine

The first example of our method is the ionization potential (IP) of pyridine, C_5H_5N . Pyridine has a π electron configuration of $(1b_2)^2(2b_2)^2(1a_2)^2$. The highest occupied molecular orbital (HOMO) $1a_2$ is a superposition of π bonding orbitals between the C_2 and C_4 atoms and between the C_5 and C_6 atoms with a negative relative phase, where the atoms are numbered by 1–6 from the N atom in clockwise order. The ionized state is well described by the configuration having an electron removed from the HOMO.

The geometry used is the (conventional) HF structure with the VDZ basis set. The IP was computed with the delta SCF and delta DFT methods, i.e. the difference between the energies of the neutral molecule and the monovalent cation. Tables 1 and 2 show the results of the PFMO HF and KS methods, respectively. The HF results are for comparison as well as for investigating the PFMO effect.

Looking at the HF results in Table 1, the total number of active MO coefficients is 3906 (for the VTZ basis set) in the neutral state, and 3813 in the ionized state. These are reduced in the PFMO to 1662 (canonical reference orbitals) and 2256 (localized reference orbitals) in the neutral state, and to 1566 (canonical reference) and 2406 (localized reference) in the ionized state. About 60% of the coefficients in the canonical reference case and 40% in the localized reference case are frozen and removed from the variational space.

Even though the variational spaces are reduced, the increase in the total energy is very small: less than one millihartree in both the neutral and ionized states. As a result, the deviation of the PFMO HF from the full HF in IP is at most 0.01 eV. We can say that the PFMO scheme with the HF method works well in this system.

Table 1. Ionization potentials for pyridine C_5NH_5 calculated with conventional and (canonical and localized reference) PFMO HF methods

VDZ	C_5NH_5		$C_5NH_5^+$		Ionization Potential ^a (eV)
	Number of active MO coefficients	Total Energy (Hartree)	Number of Variables	Total Energy (Hartree)	
Conventional HF	2688 (100%)	-246.605317	2624 (100%)	-246.322588	7.69
PFMO HF(canonical reference)	1108 (41%)	-246.604929 ^b	1056 (40%)	-246.322180	7.69
PFMO HF(localized reference)	1524 (57%)	-246.604929 ^b	1598 (61%)	-246.322084	7.70
VTZ					
Conventional HF	3906 (100%)	-246.642937	3813 (100%)	-246.364040	7.59
PFMO HF(canonical reference)	1662 (43%)	-246.642603	1566 (41%)	-246.363720	7.59
PFMO HF(localized reference)	2256 (58%)	-246.642519	2406 (63%)	-246.363714	7.59

^aAn experimental value of ionization potential for C_5NH_5 is 9.26 eV [32].

^bThe variational spaces for the canonical and localized reference cases are almost identical due to high symmetry, though the numbers of variables are different; hence very close total energies are yielded. The situation is also true of some cases in subsequent tables.

Table 2. Ionization potentials for pyridine C_5NH_5 calculated with conventional and (canonical and localized reference) PFMO KS-DFT

DZV	C_5NH_5		$(C_5NH_5)^+$		Ionization Potential ^a (eV)
	Number of active MO coefficients	Total Energy (Hartree)	Number of Variables	Total Energy (Hartree)	
Conventional KS	2688 (100%)	-248.113073	2624 (100%)	-247.800185	8.51
PFMO KS(canonical reference)	1108 (41%)	-248.106620	1056 (40%)	-247.793643	8.52
PFMO KS(localized reference)	1524 (57%)	-248.106620	1598 (61%)	-247.793661	8.52
TZV					
Conventional KS	3906 (100%)	-248.164645	3813 (100%)	-247.849585	8.57
PFMO KS(canonical reference)	1662 (43%)	-248.157093	1566 (41%)	-247.841987	8.57
PFMO KS(localized reference)	2256 (58%)	-248.156978	2406 (63%)	-247.842000	8.57

^aAn experimental value of ionization potential for C_5NH_5 is 9.26 eV [32]

Table 3. Energy difference between *cis*- and *trans*-butadiene calculated with the conventional and (canonical and localized reference) PFMO HF methods

VDZ	<i>cis</i> -butadiene		<i>trans</i> -butadiene		Energy difference ^a (kcal/mol)
	Number of active MO coefficients	Total Energy (Hartree)	Number of variables	Total Energy (Hartree)	
Conventional HF	1440 (100%)	-154.863444	1440 (100%)	-154.868966	3.47
PFMO HF(canonical reference)	680 (47%)	-154.863231	680 (47%)	-154.868753	3.47
PFMO HF(localized reference)	832 (58%)	-154.863205	840 (58%)	-154.868718	3.46
VTZ					
Conventional HF	2100 (100%)	-154.888087	2100 (100%)	-154.893851	3.62
PFMO HF (canonical reference)	1008 (48%)	-154.887886	1020 (49%)	-154.893703	3.65
PFMO HF (localized reference)	1272 (61%)	-154.887923	1260 (60%)	-154.893680	3.61

^aAn experimental value of energy difference between *cis*- and *trans*-butadiene is 2.9 kcal/mol [33].

Observing the KS-DFT results in Table 2, the reduction in the active MO coefficients is the same as in the HF case, since in both cases we used HF reference MOs in the determination of the fixing of the coefficients. One feature we can see is the increase in the total energy. In the KS-DFT case, the increase of the energy is about seven millihartrees in both states and for both basis sets. This is rather large compared to the HF case. However, the increase is uniform for the two states. The IP, therefore, shows a very small error with the PFMO KS method of only 0.01 eV, at most, which is nearly the same as that of the HF values.

The VDZ basis set gives similar results. The IP obtained with the PFMO KS method is 8.52 eV for both the canonical and localized reference MOs, which is in very good agreement with the full KS-DFT value of 8.51 eV.

The computed value of the KS-DFT of 8.57 eV (with the VTZ basis set) is 0.69 eV smaller than the experimental value of 9.26 eV [32], although it is much better than the HF value of 7.59 eV. However, this error arises from the KS-DFT method itself. We can therefore say

that the PFMO KS method also works well for this system.

Energy difference between cis- and trans-butadiene

The second example of our method is its application to the energy difference between the two isomers of butadiene. It is widely known that *trans*-butadiene is slightly more stable than the *cis*-butadiene. The energy difference is 2.9 kcal/mol according to experimental data [33]. We calculated this energy difference using the PFMO KS and HF methods. The structures used in the calculations are the (conventional) HF optimized geometries with the VDZ basis set.

Tables 3 and 4 summarize the results of the HF and KS-DFT methods, respectively. Our scheme of fixing the MO coefficients reduces the number of coefficients of the VTZ basis set from 2100 to 1008 and 1020 (for the *cis* and *trans* forms, respectively) for the canonical reference MO case, and 1272 and 1260 (for the *cis* and *trans* forms, respectively) for the localized reference MO case. The ratio of active MO coefficients is about

Table 4. Energy difference between *cis*- and *trans*-butadiene calculated with conventional and (canonical and localized reference) PFMO KS-DFT

Method	<i>cis</i> -Butadiene		<i>trans</i> -Butadiene		Energy difference ^a (kcal/mol)
	Number of active MO coefficients	Total Energy (Hartree)	Number of variables	Total Energy (Hartree)	
VDZ					
Conventional KS	1440 (100%)	-155.868278	1440 (100%)	-155.874363	3.82
PFMO KS(canonical reference)	680 (47%)	-155.863964	680 (47%)	-155.870050	3.82
PFMO KS(localized reference)	832 (58%)	-155.863888	840 (58%)	-155.869924	3.79
VTZ					
Conventional KS	2100 (100%)	-155.908797	2100 (100%)	-155.915006	3.90
PFMO KS(canonical reference)	1008 (48%)	-155.903502	1020 (49%)	-155.909891	4.01
PFMO KS(localized reference)	1272 (61%)	-155.903665	1260 (60%)	-155.909860	3.89

^aAn experimental value of the energy difference between *cis*- and *trans*-butadiene is 2.9 kcal/mol [33].

50% (canonical reference) and 60% (localized reference).

Similar to the description in the previous subsection, the increase in energy from the PFMO scheme is very small for the HF method: less than one millihartree in all the cases in Table 3. The resulting deviation from the energy difference value of the conventional HF method is also very small, at less than 0.1 kcal/mol.

The KS total energies increase from the full KS energy by 5.3 and 6.1 millihartrees (for the *cis* and *trans* forms, respectively) for the canonical reference case, and by 5.1 and 6.1 millihartrees (for the *cis* and *trans* forms, respectively) for the localized reference case. The resulting energy difference is 4.01 and 3.89 kcal/mol, for the canonical and localized reference cases, respectively. The error from the full KS-DFT result of 3.90 kcal/mol is very small. Furthermore, the agreement with the experimental value 2.9 kcal/mol is also good.

Similar results are obtained with the VDZ basis set, as discussed in the previous subsection. The energy difference obtained with the PFMO KS method is 3.82 and 3.79 kcal/mol for the canonical and localized reference cases, respectively, which are both very close to the full KS-DFT value of 3.82 kcal/mol.

Reaction barrier height for the interconversion of cyclobutene and *cis*-butadiene

The third application of our method discussed is the reaction barrier height for the interconversion of cyclobutene and *cis*-butadiene (Fig. 1). From previous studies, this system is known as one where the electron correlation is important for properly describing the bond breaking/formation (for the forward/reverse reaction) in the transition state structure [34, 35, 36, 37]. The geometries were determined by conventional DFT calculation, using the Becke 1988 exchange [27] and Lee-Yang-Parr correlation [38] functionals with the cc-pVDZ basis set.

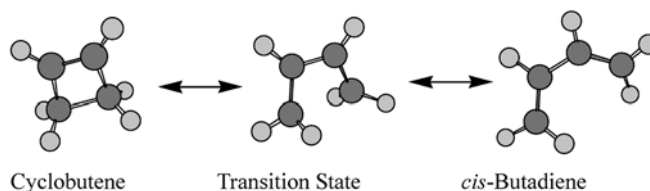


Fig. 1. The interconversion of cyclobutene and *cis*-butadiene

Table 5 shows the total energy of each structure and the barrier height at the HF level, and Table 6 shows the total energy of each structure and the barrier height at the KS-DFT level. The deviations in energy from the full HF and KS-DFT energies are similar to the previously discussed cases, at less than one millihartree for the HF case, and four to five millihartrees for the KS-DFT case. One desirable feature is that, although the ratios of the active MO coefficients are different, depending on the structures used in each PFMO method, the errors in the barrier height between the conventional and PFMO methods is 0.13 kcal/mol at most.

The electron correlation is important for an accurate description of this reaction. Experiments give the barrier height as 33 kcal/mol for the forward reaction (cyclobutene to *cis*-butadiene) [39] and 41 kcal/mol for the reverse reaction (*cis*-butadiene to cyclobutene) [33, 39, 40, 41]. The KS-DFT improves the barrier height energies to 29 and 45 kcal/mol, from the HF values of 40 and 60 kcal/mol for the forward and reverse reactions, respectively.

Hydrogen shift reaction of hydroxycarbene to formaldehyde, $\text{HCOH} \rightarrow \text{H}_2\text{CO}$

Finally, we examine another chemical reaction, the hydrogen shift reaction of hydroxycarbene to formaldehyde, along the intrinsic reaction coordinate (IRC) (Fig. 2). The geometry of the transition state (TS) as well as points on the IRC was determined by the complete active space self-consistent field method with four active

Table 5. Energy profile of the cyclobutene-*cis*-butadiene interconversion calculated with the conventional and (canonical and localized reference) PFMO HF methods

cc-pVDZ	Cyclobutene		Transition State		<i>cis</i> -Butadiene		Barrier height ^a	
	Number of active MO coefficients	Total Energy (Hartree)	Number of variables	Total Energy (Hartree)	Number of variables	Total Energy (Hartree)	cyclobutene → TS(kcal / mol)	TS → butadiene (kcal / mol)
Conventional HF	1440 (100%)	-154.830010	1440 (100%)	-154.765760	1440 (100%)	-154.861164	40.32	59.87
PFMO HF(canonical reference)	672 (47%)	-154.829799	952 (66%)	-154.765556	960 (67%)	-154.860936	40.31	59.85
PFMO HF(localized reference)	888 (62%)	-154.829799	936 (65%)	-154.765448	936 (65%)	-154.860891	40.38	59.89
cc-pVTZ								
Conventional HF	2100 (100%)	-154.861737	2100 (100%)	-154.792756	2100 (100%)	-154.884883	43.29	57.81
PFMO HF(canonical reference)	1008 (48%)	-154.861625	1428 (68%)	-154.792556	1440 (69%)	-154.884730	43.34	57.84
PFMO HF(localized reference)	1332 (63%)	-154.861625	1416 (67%)	-154.792436	1404 (67%)	-154.884640	43.42	57.86

^aAn experimental barrier height is 33 kcal/mol for cyclobutene → TS [39] and 41 kcal/mol for TS → *cis*-butadiene [33, 39, 40, 41].

Table 6. Energy profile of the cyclobutene-*cis*-butadiene interconversion calculated with conventional and (canonical and localized reference) PFMO KS-DFT

VDZ	Cyclobutene		Transition State		<i>cis</i> -Butadiene		Barrier height ^a	
	Number of active MO coefficients	Total Energy (Hartree)	Number of variables	Total Energy (Hartree)	Number of variables	Total Energy (Hartree)	cyclobutene → TS(kcal/mol)	TS → butadiene (kcal/mol)
Conventional KS	1440 (100%)	-155.844370	1440 (100%)	-155.799161	1440 (100%)	-155.872184	28.37	45.82
PFMO KS(canonical reference)	672 (47%)	-155.840017	952 (66%)	-155.794741	960 (67%)	-155.867921	28.41	45.92
PFMO KS(localized reference)	888 (62%)	-155.840017	936 (65%)	-155.794648	936 (65%)	-155.867862	28.47	45.94
VTZ								
Conventional KS	2100 (100%)	-155.885304	2100 (100%)	-155.839889	2100 (100%)	-155.910951	28.50	44.59
PFMO KS(canonical reference)	1008 (48%)	-155.880419	1428 (68%)	-155.834956	1440 (69%)	-155.905932	28.53	44.54
PFMO KS(localized reference)	1332 (63%)	-155.880419	1416 (67%)	-155.834865	1404 (67%)	-155.905865	28.59	44.55

^aAn experimental barrier height is 33 kcal/mol for cyclobutene → TS [39] and 41 kcal/mol for TS → *cis*-butadiene [33, 39, 40, 41].

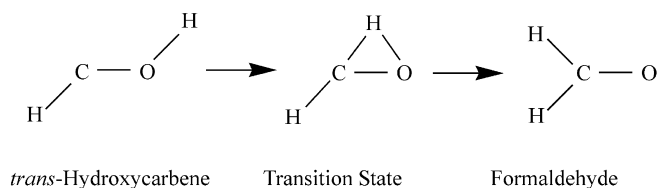


Fig. 2. The hydrogen shift reaction of hydroxycarbene of formaldehyde, $\text{HCOH} \rightarrow \text{H}_2\text{CO}$

electrons and three active orbitals. The VDZ basis set was used.

We selected 27 points for plotting the potential energy curves (PECs) along the reaction path. The ratios of the active coefficients along the IRC are 50 and 60% for the canonical and localized reference cases, respectively. For example, at the TS, the number of the active coefficients is reduced to 168 (canonical reference) and 204 (localized reference) from the original 352.

Figures 3 and 4 show the PECs at the HF and DFT levels, respectively. The PEC of the PFMO HF is almost identical to that of the full HF method, as would be expected from the results of the PFMO HF in the previous subsections. On the other hand, the PEC of the PFMO KS method is several millihartrees above that of the full KS-DFT method. However, the error is almost constant along the IRC, with the PFMO DFT keeping the shape of the PEC very well. The PFMO KS method is, therefore, also effective for chemical reactions.

Concluding remarks

We have presented a non-orthogonal KS-DFT method. The DFT energy expression for non-orthogonal orbitals was derived, and a computational scheme according to the quasi-Newton-Raphson method was given. In addition, PFMOs were introduced, which are a generalization of the ELMOs of Couty et al. In the PFMOs, only predetermined MO coefficients are active, with the other coefficients either being frozen or neglected (namely, frozen to zero). This restriction increases the electronic energy according to the variational principle. However, if the coefficients are properly restricted, the increase is small (or at least the relative energy, such as the activation energy, is small). A new procedure for restriction was also presented.

The PFMO KS method has been applied to some molecular calculations, and was compared with the conventional orthogonal KS-DFT method. A comparison between the PFMO and conventional HF methods was also made. The results were rather good. The difference between the PFMO and the conventional KS-DFT methods in the total energy was larger than that between the PFMO and the conventional HF method, almost within 0.1 millihartree in the HF case, and several millihartrees in the KS-DFT case. However, the differences in relative energy were very small, to within

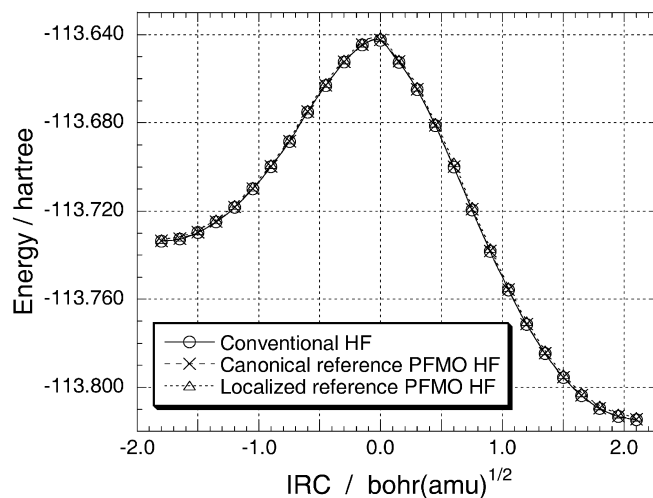


Fig. 3. The potential energy curves of $\text{HCOH} \rightarrow \text{H}_2\text{CO}$ calculated with the conventional and (canonical and localized reference) PFMO HF methods. The origin of the IRC corresponds to the TS structure at the conventional HF level

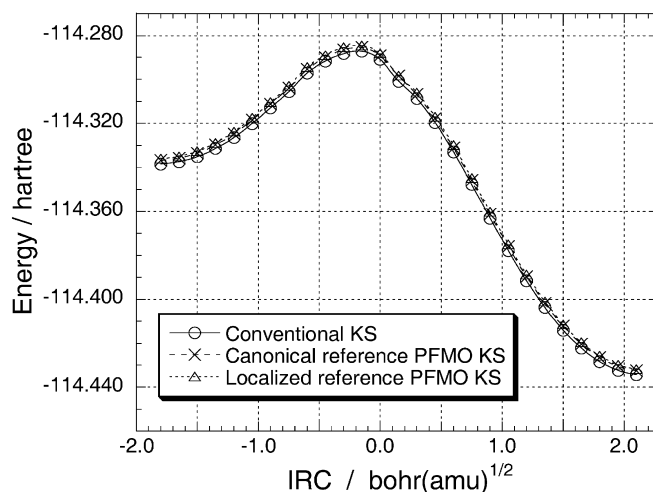


Fig. 4. The potential energy curves of $\text{HCOH} \rightarrow \text{H}_2\text{CO}$ calculated with the conventional and (canonical and localized reference) PFMO KS-DFT. The origin of the IRC corresponds to the TS structure at the conventional HF level

0.1 eV in the IP value and 0.1 kcal/mol in the barrier height and in the potential energy calculations.

Finally, we would like to make three comments on the efficiency, accuracy, and applicability of the present method.

The reduction of the active MO coefficients was 40–60%, depending on the molecular system. In all the cases studied, the number of active coefficients was larger in the localized reference orbital cases than in the canonical reference orbital cases. One reason for this is the symmetry of the canonical orbitals. The Boys localization makes the MOs lose their symmetry, increasing the non-zero values in the MO coefficients. Consequently, the ratio of active MO coefficients is smaller than for the canonical reference case. However, this feature occurs

only for small test molecules, such as those investigated in this work. In larger systems, the degree of localization is usually larger, and in this case, the localized reference orbitals will be more effective than the canonical reference orbitals. In addition, the ratio of active coefficients itself will be small in large system because of the higher possibility of localization. This implies an applicability of the localized reference orbitals to large systems.

The threshold for the frozen coefficients was set to a relatively small value to maintain the accuracy ($\delta = 0.001$). This can be relaxed if we are able to control the number of reduced MO coefficients in some way. A rough estimation of the increase in total energy is given according to the variational principle as $\Delta E \approx N \times \delta^2$, where N represents the number of reduced MO coefficients. (This is a little larger in the KS-DFT case, $\Delta E \approx c \times N \times \delta^2$, with the constant c assuming a value of being 5–10). As long as we focus on the relative energy, then we can raise the threshold by keeping $N \times \delta^2$ nearly constant. This opens up the a possibility of a more compact use of PFMOs.

The present scheme has been applied to some small single molecules. However, it can readily be extended to large systems that consist of an active reaction site and other environmental parts. Roughly, the MO coefficients on the reaction site are active, and the coefficients on the environmental parts are fixed. The non-orthogonality allows the MOs localized on the reaction site to overlap with the environmental part MOs (if active coefficients are properly selected). This degree of freedom can be a great advantage over conventional orthogonal MO methods in describing chemical reactions at the active site, where the conventional active site MOs are rather restricted by the orthogonality with the environmental part MOs. Studies along this line will be presented in future papers.

The PFMO KS method, as well as the PFMO HF method, has been implemented in a molecular electronic structure program package, UTChem [42]. All the calculations were performed using UTChem.

Acknowledgements. This research was supported in part by a Grant-in-Aid for Specially Promoted Research, "Simulations and Dynamics of Real Molecular Systems," from the Ministry of Education, Culture, Sports, Science and Technology of Japan, and a Grant-in-Aid for Scientific Research (C) to HN and a Research Fellowship for Young Scientists to TY, which were both from the Japan Society for the Promotion of Science.

References

- Saebo S, Pulay P (1993) *Annu Rev Phys Chem* 44:213
- Murphy R, Beachy B, Friesner RA, Ringnald MN (1995) *J Chem Phys* 103:1481
- Hetzer G, Pulay P, Werner H-J (1998) *Chem Phys Lett* 290:143
- Rauhut G, Pulay P, Werner H-J (1998) *J Comput Chem* 11:1241
- Schütz M, Hetzer G, Werner H-J (1999) *J Chem Phys* 111:5691
- Hetzer G, Schütz M, Stoll H, Werner H-J (2000) *J Chem Phys* 113:9443
- Lee MS, Maslen PE, Head-Gordon M (2000) *J Chem Phys* 112:3592
- Scuseria GE, Ayala PY (1999) *J Chem Phys* 111:8330
- Hampel C, Werner H-J (1996) *J Chem Phys* 104:6286
- Schütz M, Werner H-J (2001) *J Chem Phys* 114:661
- Schütz M (2000) *J Chem Phys* 113:9986
- White CA, Johnson BG, Gill PMW, Head-Gordon M (1996) *Chem Phys Lett* 253:268
- Strain MC, Scuseria GE, Frish MJ (1996) *Science* 271:51
- Challacombe M, Schwegler E, Almlöf J (1996) *J Chem Phys* 104:4685
- Challacombe M, Schwegler E (1997) *J Chem Phys* 106:5526
- White CA, Head-Gordon M (1996) *J Chem Phys* 104:2620
- Schwegler E, Challacombe M, Head-Gordon M (1997) *J Chem Phys* 106:9708
- Ochsenfeld C, White CA, Head-Gordon M (1998) *J Chem Phys* 109:1663
- Burant JC, Scuseria GE, Frisch MJ (1996) *J Chem Phys* 105:8969
- Millam JM, Scuseria GE (1997) *J Chem Phys* 106:5569
- Couty M, Bayse CA, Hall MB (1997) *Theor Chem Acc* 97:96
- Fischer TH, Almlöf J (1992) *J Phys Chem* 96:9768
- Fletcher R (1980) *Practical Methods of Optimization*, vol. 1. Wiley, New York
- Dunning TH Jr (1989) *J Chem Phys* 90:1007
- Almlöf J, Taylor PR (1990) *J Chem Phys* 92:551
- Boys SF (1960) *Rev Mod Phys* 32:296
- Becke AD (1988) *J Chem Phys* 98:5648
- Tsuneda T, Hirao K (1999) *J Chem Phys* 110:10664
- Yanagisawa S, Tsuneda T, Hirao K (2001) *J Comput Chem* 22:1995
- Yanagisawa S, Nakajima T, Tsuneda T, Hirao K (2001) *J Mol Struct (Theochem)* 537:63
- Nakano H, Nakajima T, Tsuneda T, Hirao K (2001) *J Mol Struct (Theochem)* 573:91
- El-Sayed MA, Kasha M, Tanaka Y (1960) *J Chem Phys* 34:334
- Saltiel J, Sears DF, Turek AM (2001) *J Phys Chem A* 105:7569
- Breulet J, Schaefer HF III (1984) *J Am Chem Soc* 106:1221
- Spellmeyer DC, Houk KN (1988) *J Am Chem Soc* 110:3412
- Baker J, Muir M, Andzelm J (1995) *J Chem Phys* 102, 2063
- Wiest O (1998) In: Schleyer PvR; Allinger NL, Clark T, Gasteiger J, Kollman PA, Schaefer HF III, Schreiner PR (eds) *The Encyclopedia of Computational Chemistry*, vol. 5:3104. Wiley, Chichester
- Lee C, Yang W, Parr RG (1988) *Phys Rev B* 37:785
- Cooper W, Walters WD (1958) *J Am Chem Soc* 80:4220
- Carr RW Jr, and Walters WD (1965) *J Phys Chem* 69:1073
- Wiberg KB, Fenoglio RA (1968) *J Am Chem Soc* 90, 3395
- Yanai T, Abe M, Kamiya M, Kawashima Y, Nakajima T, Nakano H, Nakao Y, Sekino H, Tsuneda T, Yanagisawa S, Hirao K (2003) *UTChem 2003*, University of Tokyo, Tokyo